

Performance assessment of adjusted nuclear data along with their covariances on the basis of fast reactor experiments

Sandro Pelloni¹, Dimitri Rochman

*Laboratory for Scientific Computing and Modeling (LSM),
Nuclear Energy and Safety Division (NES),
Paul Scherrer Institut (PSI), CH-5232 Villigen PSI, Switzerland*

Abstract

In view of fast reactor analyses, it is shown that efficient nuclear data adjustments can be obtained on a limited assimilation database consisting of just six well documented integral parameters, i.e. the central spectral indices measured in Godiva and ZPPR-9. This study uses a Generalized Linear Least-Squares (GLLS) based data assimilation method by means of Asymptotic Progressing Incremental nuclear data Adjustment (APIA) simulations with two incremental steps, one involving Godiva; the other one ZPPR-9. Consistent JEFF-3.3 and TENDL based prior data including their covariances are used; correspondingly, the assimilation leads to posterior JEFF-3.3 and TENDL data. 34 target experiments are then investigated by means of both prior and posterior data. These experiments consist of spectral indices as well as multiplication factors which pertain to 11 fast spectrum configurations including the six integral parameters which are part of the assimilation.

It is found that (1) after adjustment the mean χ^2 is strongly reduced to values smaller than 2, in each case. (2) The performance of the adjustment is comparable between JEFF-3.3 and TENDL also in terms of the Gaussian Coverage Factor (GCF), which is the common surface spanned below two normal probability density functions associated with data means and variances.

Correspondingly it is found by comparing JEFF-3.3 and TENDL data among each other in a similar way by computing GCFs of cross-sections, that (3) posterior data overall appears less deviating than prior data.

It seems worthwhile investigating whether similar promising results and trends assessed based upon a deterministic code, namely ERANOS, are reproducible with a stochastic method which is deemed to be a reference tool.

Keywords: fast-spectrum systems; JEFF-3.3 and TENDL consistent nuclear data; Asymptotic Progressing Incremental nuclear data Adjustment (APIA); Efficiency of an adjustment.

¹ Tel. +41-(0)56-310-2075; Fax: +41-(0)56-310-4411
Email address: Sandro.Pelloni@psi.ch

1. Introduction

The important task of properly assessing and reducing uncertainties of reactor parameters due to nuclear data uncertainties in a trustful way below given limits can only be achieved by ensuring that covariance data along with the basic nuclear data is obtained in a fully consistent manner. In particular all these data should stem from the same source and would also need to be processed on the basis of a consistent methodology.

This study thus addresses the task of adjusting consistent JEFF-3.3 (Nuclear Energy Agency (NEA), 2018) and TENDL (Koning and Rochman, 2012) based data along with their covariances in the fast energy range; the Asymptotic Progressing Incremental nuclear data Adjustment (APIA) methodology proposed in (Pelloni and Rochman, 2018) is used. At this point it is worthwhile mentioning that JEFF-3.3 is already partly adjusted to integral data.

Section 2 deals with general considerations describing the benchmark case and the experimental database for the assimilation, Section 2.1; Section 2.2 is devoted to APIA features in addition to specific refinements of the methodology; thus enabling to compare adjustments in general terms. Section 3 is dedicated to extensive analyses of the results in particular comparisons of JEFF-3.3 and TENDL data primarily in terms of their performance in analyzing a series of benchmarks. Finally, Section 4 summarizes the main findings, provides conclusions and points on key recommendations for future work.

2. General considerations

The Asymptotic Progressing Incremental nuclear data Addjustment (APIA) methodology (Pelloni and Rochman, 2018) is used to assimilate a small number of relevant experimental data of central spectral indices, Section 2.1. The aim of the study is that of analyzing by means of the resulting adjusted data, i.e. posterior data along with their covariances, several target experiments for fast reactor applications with the majority of these experiments outside the assimilation process, and to compare the results with those obtained based upon unadjusted data, i.e. prior data along with their covariances.

It is recalled (Pelloni and Rochman, 2018) that the main idea lying behind the APIA approach is that the adjustment is made progressively in subsequent steps, by considering at a time small groups of well documented experiments possibly with low experimental uncertainties, which have been performed in the same configuration.

The envisaged target experiments include integral parameters considered in the framework of the International “Subgroup 39” on “Methods and approaches to provide feedback from nuclear and covariance data adjustment for improvement of nuclear data files” of the Working Party on Evaluation Cooperation (WPEC) of the OECD Nuclear Energy Agency Nuclear Science Committee (NSC) (Salvatores et al., 2014). As in (Pelloni and Rochman, 2018) the adjustment is performed for the ten most important nuclides of the benchmarks in view of neutronics analyses. These nuclides are ^{16}O , ^{23}Na , ^{52}Cr , ^{56}Fe , ^{58}Ni , ^{235}U , ^{238}U , ^{239}Pu , ^{240}Pu and ^{241}Pu ; thus consistently with (Salvatores et al., 2014), not including ^{237}Np . Adjusted are six data types i.e. elastic and inelastic scattering, lumped (n, 2n) and (n, 3n) named (n, xn), capture and fission cross-sections, as well as \bar{v} .

In order to avoid inconsistencies (Pelloni and Rochman, 2018) the adjustment is obtained by solely using prior data stemming from the same data source in terms of cross-sections and their covariances, which is JEFF-3.3 (Nuclear Energy Agency (NEA), 2018) and TENDL (Koning and Rochman, 2012). While TENDL data was generated in-house on the basis of available random files produced for the different nuclides (Koning and Rochman, 2008), JEFF-3.3 covariances were generated at the NEA Data Bank and then distributed to the “Subgroup 39” members in different dedicated formats. This covariance data has originally been processed with NJOY (MacFarlane et al., 2012) from ENDF formatted files.

The deterministic code system ERANOS (Edition 2.2-N) (Rimpault et al., 2002) is then used in the framework of the APIA simulations to compute all required neutronic parameters including uncertainties due to nuclear data uncertainties, by using P_1S_{16} approximations in the required forward and adjoint transport-theory calculations. As in previous studies e.g. (Pelloni and Rochman, 2018), fission spectra, secondary energy/angular distributions, background cross-section (σ_0) dependences, and data for nuclides other than those aforementioned and thus remaining unadjusted, all are stemming from the original JEFF-3.1 based ERANOS library.

2.1 Experimental database

More precisely, the current assimilation accounts for central core measurements of spectral indices carried out in two configurations, Godiva and ZPPR-9. The APIA simulations performed with data in 33 neutron groups (Rimpault et al., 2002) dealt with in this study correspondingly use two incremental steps. In a previous analysis considering a larger number of steps (Pelloni and Rochman, 2018) it has namely been ascertained that the assimilation of this experimental data is responsible for significant adjustments of U235 (Godiva), respectively of U238 and Pu239 data (ZPPR-9). Also, APIA simulations with different sequences using consistent prior data in terms of the same data source for the data along with their covariances were found able providing similarly adjusted cross-sections and equal posterior sensitivity coefficients. Correspondingly, conflicting effects on adjusted cross-sections between individual incremental steps e.g. increases followed by larger decreases than the increases reversing the trend, which were found to appear especially when using inconsistent data, are largely avoided; all these characteristics indicative of consistent adjustments, along with the consideration of just a few well documented experiments, constitute the basis for the current choice of the assimilation database.

34 target experiments performed in 11 configurations are analyzed with (1) unadjusted data i.e. prior data along with their covariances, and then (2) adjusted data i.e. posterior data along with their covariances, in order to test along with the unadjusted data, the individual adjustments by comparing the performance of the JEFF-3.3 and TENDL based data in a consistent manner, Section 2.2.

These experiments include the 6 parameters which are part of the assimilation supplemented by a larger number of experimental data which are not assimilated, namely 28, Table 1.

The current selection criterion for the target experiments is primarily given by the availability in the ICSBEP (Briggs, 2004) and IRPhEP (Nuclear Energy Agency (NEA), 2017) collections, of configurations in which spectral indices were measured. Due to the limitation to $P_0 - P_1$ scattering in the current ERANOS calculations (Pelloni, 2014), the effective multiplication factor of the envisaged metal systems is not considered.

It is anticipated that the adjustment of $\bar{\nu}$ is quite small because the database for assimilations is limited to spectral indices having weak sensitivities to $\bar{\nu}$.

k_{eff} , a parameter which is not assimilated (Pelloni, 2017), as usually refers to the effective multiplication factor. The abbreviations $F28$, $F25$, $F49$, and $F37$ are respectively used for ^{238}U , ^{235}U , ^{239}Pu , and ^{237}Np fission reaction rates per atom; $C28$ denotes the ^{238}U capture reaction rate per ^{238}U atom.

For general understanding, the individual configurations are briefly characterized (Briggs, 2004), (Nuclear Energy Agency (NEA), 2017) hereafter. It is recalled that

Godiva is a bare sphere consisting of 94 weight% U235 enriched U. The experimental data, a part of which is used in the current assimilation, was obtained in Los Alamos, USA.

U235 Flattop is a spherical, highly enriched U core reflected by natural U. The experiments were conducted in Los Alamos.

Big Ten is a large mixed U metal cylindrical core with 10% average U235 enrichment, surrounded by a thick U238 reflector. The experiments were conducted in Los Alamos.

Pu239 Jezebel is a bare sphere of Pu239 with 4.5 atom% Pu240 and 1.02 weight% Ga. The experiments were conducted in Los Alamos.

Pu240 Jezebel is a bare sphere of Pu239 with 20.1 atom% Pu240 and 1.01 weight% Ga. The experiments were conducted in Los Alamos.

Pu239 Flattop is a spherical Pu239 core reflected by natural U. The experiments were conducted in Los Alamos.

ZPPR-9 is a zero-power mockup of a large pancake like sodium-cooled fast breeder reactor core with conventional Mixed OXide (MOX) fuel. The experimental data, a part of which is also used in the current assimilation, was obtained under a joint research program between the U.S. Deartment Of Energy (DOE) and the Japanese Power Reactor and Nuclear Fuel Development Corporation (PNC), the former name of the Japan Nuclear Cycle Development Institute (JNC).

ZPR-6/7 simulates a large sodium-cooled fast breeder reactor fueled with MOX having a ratio of active core height over diameter of nearly one. The experiments were conducted at the Argonne National Laboratory (ANL), USA.

JOYO MK-I 64 F/A is the first Japanese experimental fast breeder reactor (50 MW) operating with MOX fuel with enriched U. It was constructed at the O-arai Engineering Center (OEC) of PNC.

SNEAK 7A and SNEAK 7B are zero-power facilities with one-zone cores of MOX fuel with natural U, reflected by depleted U. The unit cell of SNEAK 7A consists of one MOX platelet (26.6% PuO₂ containing 8% Pu240) and one graphite platelet. In SNEAK 7B the graphite platelet is replaced by a UO₂ platelet reducing the Pu content of U + Pu to 13%. The experiments were conducted in the Fast Zero-Power Facility in Karlsruhe, Germany.

Table 1: Target parameters

| Configuration | | Integral parameters | Part of the data assimilation (Yes/No) |
|--|--------------------|--------------------------------------|--|
| Metal systems ^a | | | |
| Name | ICSBEP identifier | | |
| U based | | | |
| Godiva | HEU-MET-FAST-001 | $F28/F25, F49/F25, F37/F25$ | Yes |
| U235 Flattop | HEU-MET-FAST-028 | $F28/F25, F49/F25, F37/F25$ | No |
| Big Ten | IEU-MET-FAST-007 | $F28/F25, F49/F25, F37/F25, C28/F25$ | |
| Pu based | | | |
| Pu239 Jezebel | PU-MET-FAST-001 | $F28/F25, F49/F25, F37/F25$ | |
| Pu240 Jezebel | PU-MET-FAST-002 | $F28/F25, F37/F25$ | |
| Pu Flattop | PU-MET-FAST-006 | $F28/F25, F37/F25$ | |
| Compound systems with sodium ^b | | | |
| Name | IRPhEP identifier | | |
| ZPPR-9 | ZPPR-LMFR-EXP-002 | $F28/F25, F49/F25, C28/F25$ | Yes |
| ZPPR-9 | ZPPR-LMFR-EXP-002 | k_{eff} | No |
| ZPR-6/7 | ZPR-LMFR-EXP-001 | $F28/F25, F49/F25, C28/F25, k_{eff}$ | |
| JOYO MK-I 64 F/A | JOYO-LMFR-RESR-001 | k_{eff} | |
| Compound systems without sodium ^b | | | |
| SNEAK 7A | SNEAK-LMFR-EXP-001 | $F28/F25, F49/F25, C28/F25, k_{eff}$ | No |
| SNEAK 7B | SNEAK-LMFR-EXP-001 | $F28/F25, F49/F25, C28/F25, k_{eff}$ | |

^a According to the International Handbook of Evaluated Criticality Safety Benchmark Experiments (International Criticality Safety Benchmark Evaluation Project, ICSBEP), (Briggs, 2004)

^b According to the International Handbook of Evaluated Reactor Physics Benchmark Experiments (International Reactor Physics Evaluation Project, IRPhEP), (Nuclear Energy Agency (NEA), 2017)

2.2 Data adjustment features

Differently from (Pelloni and Rochman, 2018) the convergence of the individual APIA steps is significantly tightened by requiring that the maximum relative cross-section difference between two successive within step iterations becomes in magnitude very small in the order of 0.01%, instead of 1% , requiring a number of

iterations in the range of 100 in this specific case, warranting full convergence. Due to the sequence independence of the adjusted data, the refined convergence criterion ensures that the ratios C/E s of the computed (C) posterior values to experimental (E) values approach more closely unity as compared to the previous study for the experimental integral parameters being assimilated.

After completion of the full APIA simulation the posterior covariance data is reassessed in order to avoid multiple consideration of the experimental information used in the assimilation. By associating index s with APIA step s with $s = 0$ and $s = nstep$ respectively for the prior situation and the last incremental step, with $nstep = 2$ in this study; the posterior covariance matrix M_{nstep} is recomputed based upon the following recursive equation:

$$M_{s+1} = (M_{s+1,j,j'}) = M_s - M_s G_{s+1,\infty}^T (G_{s+1,\infty} M_s G_{s+1,\infty}^T + V_E + V_M)^{-1} G_{s+1,\infty} M_s; \quad (1)$$

$s = 0, 1, \dots, nstep - 1$

In Eq. (1) the superscripts T and -1 respectively indicate matrix transpose and inversion. $G_{s+1,\infty}$ is the matrix of the converged asymptotic explicit sensitivity coefficients resulting from the data adjustment provided by APIA step ($s + 1$); V_E and V_M are the usual experimental, respectively analytical modeling covariance matrix (Salvatores, M. et al., 2014).

It is proposed that the C -values, a set of computed arithmetic means, along with their uncertainties due to nuclear data uncertainties, ΔC s, in fact one-sigma standard deviations or square roots of variances, are systematically compared with the corresponding benchmark values, E s, i.e. means having variances corresponding to the experimental uncertainties, ΔE s. The comparison is carried out in terms of Coverage Factors, CFs, knowing the correct Probability Density Functions, PDFs. The PDFs are required to have these means and variances; while the experimental data can be assumed normally distributed, the PDFs associated with the C s are not necessarily symmetric (Rochman et al., 2018).

By doing in this way, nuclear data along with their uncertainties and eventually cross-correlations are viewed as an inseparable, unique entity.

More specifically, the CF of two data sets consisting each of one mean along with its variance, a number between 0 and 1, is nothing else than the common surface spanned below probability density functions associated with each set having these means and variances. The larger is this number the better is the agreement of the two data sets, which is thus not judged simply on the basis of the difference of the means. In the limiting cases, perfect agreement is achieved when $CF = 1$ meaning identical means along with fully matching PDFs, whereas no agreement, i.e. no common surface, is the result of $CF = 0$. For simplicity, in the whole discussion, the CF will be referred to as coverage factor of the means.

It is claimed that the more suited is the adjustment i.e. the better is its performance, the larger is the mean coverage factor of computed and experimental values taken over suited target parameters, which is reached in the posterior situation. A heuristic explanation of this relationship is that independently of the specific adjustment methodology, the posterior data resulting from assimilations should account as much as possible for the precise knowledge of experimental data along with their bias and eventually their cross-correlations. In other words, specific adjusted data along with their covariances should directly result from the experimental information used in the assimilation with the capability of reproducing this information with high fidelity in the posterior situation, except maybe for methodological uncertainties. In the current APIA simulations this requirement is largely fulfilled on the basis of the enhanced data convergence achieved within the iterative scheme.

Whereas prior CFs of C - and E -values are judged less valuable and will thus not be reported, since (unadjusted) uncertainties of nuclear data ideally should be largely uncorrelated with uncertainties of experimental integral parameters.

Because on the one hand the APIA methodology largely makes use of the Generalized Linear Least-Squares (GLLS) approach and the current uncertainty calculations, on the other hand, use the “sandwich rule” based upon sensitivity coefficients i.e. first-order error propagation (Cacuci, 2010), it is legitimated to assume normal, hence symmetric PDFs also in the case of the computed values. Correspondingly, the specific coverage factors dealt with in this study are called Gaussian Coverage Factors (GCFs).

A clarifying example is provided in Fig. 1.

In the most optimistic hypothetical situation the use of posterior data would lead systematically to C/E s of 1 i.e. to a mean χ^2 of 0, along with matching uncertainties due to nuclear data uncertainties with experimental uncertainties, resulting in a mean GCF of exactly one. It is worthwhile underlining that on the basis of the proposed criterion of comparing CFs rather than C/E s, lower posterior χ^2 s are not necessarily characterizing better adjustments, e.g. in cases where posterior uncertainties due to nuclear data uncertainties would be much smaller than experimental uncertainties, Fig. 2: the coverage of the blue and black or experimental PDF curve, normal distributions, is larger than the coverage of red and black PDFs having identical means.

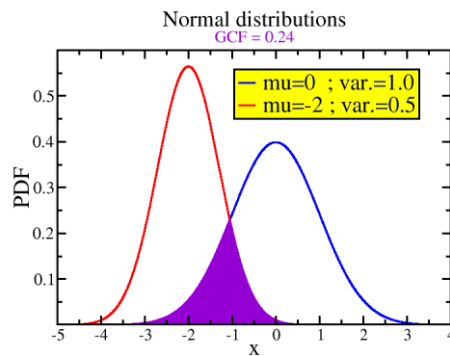


Fig. 1: GCF, an example: “mu” and “var.” are respectively means and variances of the PDFs

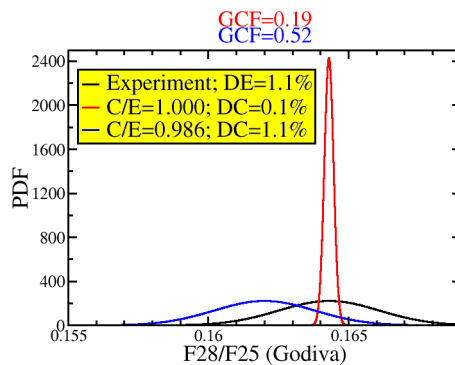


Fig. 2: Example of normal distributions for hypothetical situations

3. Discussion of the results

Data convergence achieved in the current APIA simulations, Section 2, is demonstrated in Fig. 3 on the illustrative basis of the fission cross-section of U235 in the energy range between 302keV and 183keV.

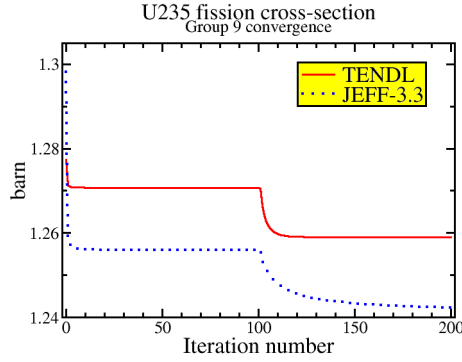


Fig. 3: Data adjustment, example

The first 100 iterations reducing this cross-section i.e. “Iteration 1” to “Iteration 100”, “Iteration 0” pointing to the prior situation, refer to the first assimilation step of the Godiva experimental spectral indices; whereas iterations 100-200 leading to a further, non-contradictory cross-section decrease, deal with the second step in which ZPPR-9 spectral indices are assimilated, Table 1. In fact “Iteration 100” which reflects the posterior situation of the assimilation of the Godiva spectral indices, also corresponds to the prior situation of this second step, and last “Iteration 200” refers to the final posterior data.

Differences between posterior and prior cross-sections are of similar magnitude i.e. 0.02 barn. However, the prior JEFF-3.3 cross-section is larger than the TENDL cross-section, while, on the contrary, the posterior cross-section is smaller, which reflects a stronger adjustment obtained with JEFF-3.3 data for this specific cross-section.

The iterative standard deviation which of course is just one datum used in the current APIA simulations to determine the overall adjustment, is correspondingly provided in relative terms in Fig. 4 showing its convergence. The asymptotic value, respectively of 0.016 and 0.006 in the case of JEFF-3.3 and TENDL data, is then reassessed according to Eq. (1) and found resulting in slight increases to 0.021 and 0.008.

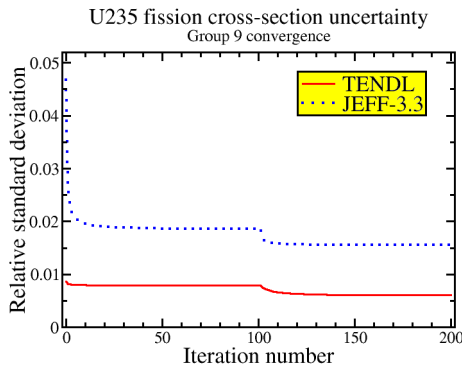


Fig. 4: Covariance data adjustment, example

Comparing these last two figures indicates that the adjustment is in the order of one prior standard deviation, in each case.

Fig. 5 displays corresponding PDFs indicating that for the fission cross-section of U235 in the energy range between 302keV and 183keV the GCF of JEFF-3.3 and TENDL data is increased through the assimilation (thicker versus thinner curves), which is equivalent to say that the “distance” (Varet et al., 2015) between JEFF-3.3 and TENDL is reduced: the JEFF-3.3 and TENDL posterior cross-sections are thus judged in better agreement among each other than the corresponding prior cross-sections, and this although as indicated, the cross-section differences are of similar magnitude.

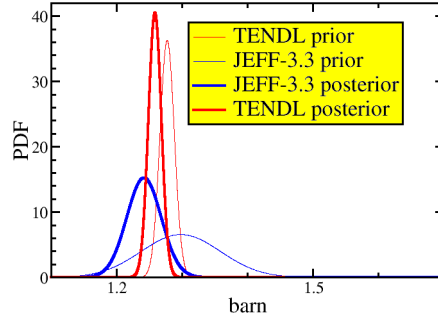


Fig. 5: U235 fission cross-section, group 9

Fig. 6 displays energy-dependent fission cross-sections of U235 in the whole energy domain being considered which is between 20MeV and 1keV. The domain is split into three ranges to better distinguish the various data.

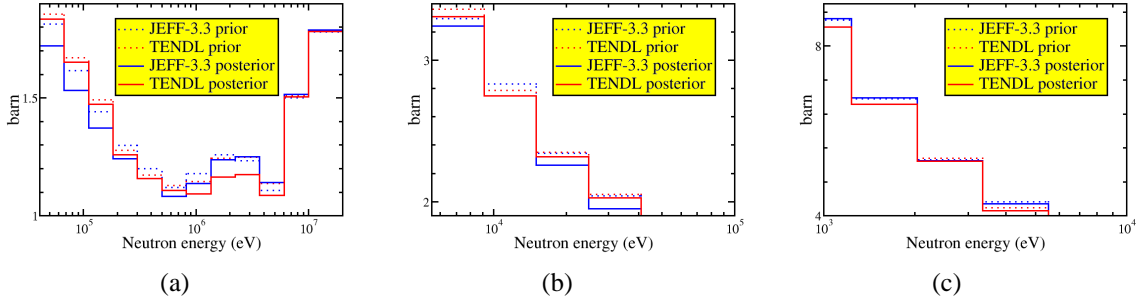


Fig. 6: U235 fission cross-section: (a) groups 1-12; (b) groups 13-16; (c) groups 17-20

The figure shows that the adjustment is not unique. In particular, differences between posterior JEFF-3.3 and TENDL data (solid curves) may be larger than corresponding differences of prior data (dotted curves) and different trends may appear for adjacent groups.

Table 2 gives prior and posterior simplified χ^2 s for the target parameters, see Table 1. For a single parameter the following definition is used:

$$\chi^2 = \left(\frac{C - E}{\Delta E} \right)^2 \quad (2)$$

In practice, since ΔE covers the interval of one standard deviation, a value of χ^2 smaller than or equal to 1 indicates that the computed value, C , agrees satisfactorily with the experimental value, E , within one standard deviation corresponding to a probability of 68.2%.

The simplified χ^2 is independent of the uncertainty, ΔC , due to nuclear data uncertainties.

Table 2: χ^2 s for target parameters along with arithmetic means

| Configuration | Integral parameter | χ^2 | | | |
|----------------------------|--------------------|----------|-----------|-------|-----------|
| | | JEFF-3.3 | | TENDL | |
| | | Prior | Posterior | Prior | Posterior |
| Godiva | <i>F28/F25</i> | 0.7 | 0.0 | 42.4 | 0.0 |
| | <i>F49/F25</i> | 3.9 | 0.0 | 5.1 | 0.0 |
| | <i>F37/F25</i> | 3.7 | 0.0 | 7.8 | 0.0 |
| | Mean | 4.8 | 0.0 | 18.4 | 0.0 |
| U235 Flattop | <i>F28/F25</i> | 7.6 | 0.0 | 44.4 | 0.4 |
| | <i>F49/F25</i> | 3.0 | 0.5 | 4.9 | 0.0 |
| | <i>F37/F25</i> | 1.6 | 0.7 | 5.3 | 0.2 |
| | Mean | 4.1 | 0.4 | 18.2 | 0.2 |
| Big Ten | <i>F28/F25</i> | 57.4 | 2.9 | 138.6 | 10.0 |
| | <i>F49/F25</i> | 3.6 | 9.3 | 15.1 | 3.9 |
| | <i>F37/F25</i> | 6.3 | 9.3 | 17.2 | 0.0 |
| | <i>C28/F25</i> | 9.7 | 2.0 | 1.8 | 2.0 |
| | Mean | 19.3 | 5.9 | 43.2 | 3.9 |
| Pu239 Jezebel | <i>F28/F25</i> | 14.0 | 4.6 | 37.0 | 0.0 |
| | <i>F49/F25</i> | 4.0 | 0.3 | 4.2 | 0.8 |
| | <i>F37/F25</i> | 0.6 | 0.1 | 0.8 | 4.2 |
| | Mean | 6.2 | 1.7 | 14.0 | 1.7 |
| Pu240 Jezebel | <i>F28/F25</i> | 20.9 | 7.5 | 46.5 | 0.3 |
| | <i>F37/F25</i> | 1.0 | 5.0 | 1.1 | 20.1 |
| | Mean | 10.9 | 6.2 | 23.8 | 10.2 |
| Pu Flattop | <i>F28/F25</i> | 18.4 | 4.0 | 45.5 | 0.7 |
| | <i>F37/F25</i> | 0.4 | 1.1 | 0.8 | 3.5 |
| | Mean | 9.4 | 2.5 | 23.2 | 2.1 |
| ZPPR-9 | <i>F28/F25</i> | 2.8 | 0.0 | 11.3 | 0.0 |
| | <i>F49/F25</i> | 0.4 | 0.0 | 1.0 | 0.0 |
| | <i>C28/F25</i> | 3.0 | 0.0 | 0.0 | 0.0 |
| | k_{eff} | 46.1 | 1.6 | 7.5 | 7.1 |
| | Mean | 13.1 | 0.4 | 5.0 | 1.8 |
| ZPR-6/7 | <i>F28/F25</i> | 0.2 | 4.0 | 1.6 | 3.7 |
| | <i>F49/F25</i> | 2.5 | 0.9 | 3.7 | 0.9 |
| | <i>C28/F25</i> | 1.1 | 0.1 | 0.0 | 0.0 |
| | k_{eff} | 14.1 | 0.5 | 11.4 | 0.5 |
| | Mean | 4.5 | 1.4 | 4.2 | 1.3 |
| JOYO MK-I 64 F/A | k_{eff} | 1.3 | 0.8 | 8.2 | 0.0 |
| SNEAK 7A | <i>F28/F25</i> | 5.4 | 1.6 | 11.3 | 1.5 |
| | <i>F49/F25</i> | 1.9 | 0.7 | 1.9 | 0.6 |
| | <i>C28/F25</i> | 4.5 | 1.2 | 1.6 | 1.3 |
| | k_{eff} | 3.5 | 0.3 | 4.7 | 0.3 |
| | Mean | 3.8 | 0.9 | 4.9 | 0.9 |
| SNEAK 7B | <i>F28/F25</i> | 3.5 | 0.0 | 15.8 | 0.3 |
| | <i>F49/F25</i> | 0.3 | 0.5 | 1.0 | 0.0 |
| | <i>C28/F25</i> | 1.3 | 0.0 | 0.0 | 0.0 |
| | k_{eff} | 3.4 | 0.0 | 0.3 | 0.3 |
| | Mean | 2.1 | 0.1 | 4.3 | 0.2 |
| Mean of target experiments | | 4.1 | 1.7 | 14.7 | 1.8 |

By associating for the time being higher performances with lower χ^2 s, it may be deduced that

- (1) Using JEFF-3.3 data appears more suited in the prior situation, with the exceptions of $C28/F25$ and k_{eff} for ZPPR-9, ZPR-6/7 and SNEAK 7B. However, the prior mean χ^2 s of all 34 experiments are found much larger than one in each case.
- (2) The agreeing posterior values characterizing similar performances are much closer to one, indicating particularly efficient adjustments in spite of the limited assimilation database, especially for TENDL data having a larger prior χ^2 . As targeted, Section 2.2, the posterior χ^2 s of the individual integral parameters which are part of the assimilation do all coincide with 0 (C/E s equal to 1) due to tight convergence reached in the two APIA simulations; larger posterior χ^2 s relatively to the overall mean are observed for Pu240 Jezebel and Big Ten.

In the following, GCFs of C - and E -values are compared to the χ^2 s: separate tables are given for the individual configurations including in addition to ratios of calculated to experimental values, C/E s, the benchmark and computed values, E s and C s, along with their standard deviations ΔE s (Briggs, 2004), (Nuclear Energy Agency (NEA), 2017) and ΔC s, which are respectively resulting from experimental/modeling and nuclear data uncertainties. It is recalled, Section 2.2, that GCFs are claimed to be meaningful only in the posterior situation.

For Godiva taking part in the assimilation, GCFs found in the order of 0.9, Table 3, highlight that the computed posterior uncertainties due to nuclear data uncertainties are largely in agreement with the experimental uncertainties.

Table 3: Godiva results

| $C/E \rightarrow$ Integral parameter \downarrow | Prior | | Posterior | |
|--|----------|-------|-----------|-------|
| | JEFF-3.3 | TENDL | JEFF-3.3 | TENDL |
| $F28/F25$ | 0.971 | 0.929 | 1.000 | 1.000 |
| $F49/F25$ | 0.980 | 0.978 | 1.000 | 1.000 |
| $F37/F25$ | 0.973 | 0.961 | 1.000 | 1.000 |
| χ^2 | 4.8 | 18.4 | 0.0 | 0.0 |
| GCF | | | 0.91 | 0.87 |

| Integral parameter | Benchmark $E \pm \Delta E$ | | | Prior $C \pm \Delta C$ | | Posterior $C \pm \Delta C$ | |
|--------------------|----------------------------|------------|------------|------------------------|----------|----------------------------|----------|
| | E | ΔE | | C | JEFF-3.3 | TENDL | JEFF-3.3 |
| $F28/F25$ | E | 0.16430 | C | 0.15959 | 0.15258 | 0.16431 | 0.16430 |
| | ΔE | 0.00180 | ΔC | 0.00573 | 0.00370 | 0.00172 | 0.00162 |
| $F49/F25$ | E | 1.41520 | C | 1.38746 | 1.38365 | 1.41511 | 1.41591 |
| | ΔE | 0.01400 | ΔC | 0.03058 | 0.02458 | 0.01096 | 0.01178 |
| $F37/F25$ | E | 0.85160 | C | 0.82867 | 0.81809 | 0.85154 | 0.85175 |
| | ΔE | 0.01200 | ΔC | 0.02015 | 0.01355 | 0.00913 | 0.00687 |

For U235 Flattop which is not part of the assimilation, the adjustment is though particularly efficient for $F28/F25$ in conjunction with TENDL data, Table 4. Noticeable is the equivalent GCF (0.77) in spite of the markedly larger prior χ^2 obtained using TENDL data.

Table 4: U235 Flattop results

| $C/E \rightarrow$ Integral parameter \downarrow | Prior | | Posterior | |
|--|----------|-------|-----------|-------|
| | JEFF-3.3 | TENDL | JEFF-3.3 | TENDL |
| $F28/F25$ | 0.970 | 0.929 | 0.999 | 0.994 |
| $F49/F25$ | 0.985 | 0.981 | 1.006 | 1.002 |
| $F37/F25$ | 0.984 | 0.970 | 1.011 | 1.006 |
| χ^2 | 4.1 | 18.2 | 0.4 | 0.2 |
| GCF | | | 0.77 | 0.77 |

| Integral parameter | Benchmark $E \pm \Delta E$ | | | Prior $C \pm \Delta C$ | | Posterior $C \pm \Delta C$ | |
|--------------------|-------------------------------|---------|------------|---------------------------|---------|-------------------------------|---------|
| | | | | JEFF-3.3 | TENDL | JEFF-3.3 | TENDL |
| | | | | $F28/F25$ | E | 0.14920 | C |
| | ΔE | 0.00160 | ΔC | 0.00453 | 0.00286 | 0.00148 | 0.00130 |
| $F49/F25$ | E | 1.38470 | C | 1.36401 | 1.35812 | 1.39315 | 1.38695 |
| | ΔE | 0.01200 | ΔC | 0.03226 | 0.02325 | 0.01153 | 0.01125 |
| $F37/F25$ | E | 0.78040 | C | 0.76761 | 0.75727 | 0.78906 | 0.78479 |
| | ΔE | 0.01000 | ΔC | 0.01789 | 0.01046 | 0.00895 | 0.00564 |

For Big Ten, Table 5, efficient adjustment is also observed for $F28/F25$; the lower GCF as compared to the other U235 based metal systems is reflected in stronger deviating posterior ΔC s from the ΔE s.

Table 5: Big Ten results

| $C/E \rightarrow$ Integral parameter \downarrow | Prior | | Posterior | |
|--|----------|-------|-----------|-------|
| | JEFF-3.3 | TENDL | JEFF-3.3 | TENDL |
| $F28/F25$ | 0.931 | 0.893 | 0.985 | 0.971 |
| $F49/F25$ | 0.987 | 0.973 | 1.022 | 0.986 |
| $F37/F25$ | 0.977 | 0.961 | 1.028 | 0.999 |
| $C28/F25$ | 0.915 | 0.963 | 0.961 | 0.962 |
| χ^2 | 19.3 | 43.2 | 5.9 | 3.9 |
| GCF | | | 0.38 | 0.47 |

| Integral parameter | Benchmark $E \pm \Delta E$ | | | Prior $C \pm \Delta C$ | | Posterior $C \pm \Delta C$ | |
|--------------------|-------------------------------|---------|------------|---------------------------|---------|-------------------------------|---------|
| | | | | JEFF-3.3 | TENDL | JEFF-3.3 | TENDL |
| | | | | $F28/F25$ | E | 0.03739 | C |
| | ΔE | 0.00034 | ΔC | 0.00173 | 0.00066 | 0.00123 | 0.00055 |
| $F49/F25$ | E | 1.19360 | C | 1.17763 | 1.16098 | 1.21927 | 1.17710 |
| | ΔE | 0.00840 | ΔC | 0.04908 | 0.02184 | 0.02005 | 0.01415 |
| $F37/F25$ | E | 0.32230 | C | 0.31474 | 0.30986 | 0.33144 | 0.32206 |
| | ΔE | 0.00300 | ΔC | 0.01650 | 0.00390 | 0.01054 | 0.00356 |
| $C28/F25$ | E | 0.11000 | C | 0.10066 | 0.10596 | 0.10574 | 0.10580 |
| | ΔE | 0.00300 | ΔC | 0.00523 | 0.00154 | 0.00266 | 0.00134 |

For Pu239 Jezebel, a Pu based metal system which is not part of the assimilation; the adjustment is efficient except for $F37/F25$ in conjunction with TENDL data, Table 6. However, Np237 has not been adjusted. There is overall agreement between posterior ΔC s and ΔE s.

Table 6: Pu239 Jezebel results

| $C/E \rightarrow$ Integral parameter \downarrow | Prior | | Posterior | |
|--|----------|-------|-----------|-------|
| | JEFF-3.3 | TENDL | JEFF-3.3 | TENDL |
| $F28/F25$ | 0.959 | 0.933 | 0.976 | 1.001 |
| $F49/F25$ | 0.982 | 0.982 | 0.995 | 1.008 |
| $F37/F25$ | 0.990 | 0.987 | 1.005 | 1.029 |
| χ^2 | 6.2 | 14.0 | 1.7 | 1.7 |
| GCF | | | 0.62 | 0.60 |

| Integral parameter | Benchmark $E \pm \Delta E$ | | | Prior $C \pm \Delta C$ | | Posterior $C \pm \Delta C$ | |
|--------------------|-------------------------------|---------|------------|---------------------------|---------|-------------------------------|---------|
| | | | | JEFF-3.3 | TENDL | JEFF-3.3 | TENDL |
| $F28/F25$ | E | 0.21330 | C | 0.20453 | 0.19903 | 0.20824 | 0.21348 |
| | ΔE | 0.00230 | ΔC | 0.00678 | 0.00470 | 0.00347 | 0.00311 |
| $F49/F25$ | E | 1.46090 | C | 1.43465 | 1.43408 | 1.45393 | 1.47270 |
| | ΔE | 0.01300 | ΔC | 0.02579 | 0.02865 | 0.01202 | 0.01480 |
| $F37/F25$ | E | 0.98350 | C | 0.97321 | 0.97104 | 0.98845 | 1.01175 |
| | ΔE | 0.01400 | ΔC | 0.01730 | 0.01812 | 0.00831 | 0.01143 |

The results for Pu240 Jezebel, Table 7, are similar to Pu239 Jezebel as regards $F28/F25$. However, the adjustment is seen causing degradation for $F37/F25$; resulting in lower GCFs. Worthwhile noticing is that the larger posterior χ^2 for TENDL as compared to JEFF-3.3 data (10.2 versus 6.2) is associated with an also larger GCF (0.38 versus 0.23), pointing on better agreement reached by means of TENDL data between posterior ΔC s and ΔE s as confirmed by the data available in the lower part of the table.

Table 7: Pu240 Jezebel results

| $C/E \rightarrow$ Integral parameter \downarrow | Prior | | Posterior | |
|--|----------|-------|-----------|-------|
| | JEFF-3.3 | TENDL | JEFF-3.3 | TENDL |
| $F28/F25$ | 0.954 | 0.931 | 0.972 | 1.006 |
| $F37/F25$ | 1.014 | 1.015 | 1.031 | 1.062 |
| χ^2 | 10.9 | 23.8 | 6.2 | 10.2 |
| GCF | | | 0.23 | 0.38 |

| Integral parameter | Benchmark $E \pm \Delta E$ | | | Prior $C \pm \Delta C$ | | Posterior $C \pm \Delta C$ | |
|--------------------|-------------------------------|---------|------------|---------------------------|---------|-------------------------------|---------|
| | | | | JEFF-3.3 | TENDL | JEFF-3.3 | TENDL |
| $F28/F25$ | E | 0.20710 | C | 0.19751 | 0.19279 | 0.20136 | 0.20828 |
| | ΔE | 0.00210 | ΔC | 0.00669 | 0.00458 | 0.00351 | 0.00318 |
| $F37/F25$ | E | 0.93650 | C | 0.94972 | 0.95039 | 0.96563 | 0.99474 |
| | ΔE | 0.01300 | ΔC | 0.01782 | 0.01763 | 0.00874 | 0.01165 |

The Pu Flattop results, Table 8, showing once again efficient adjustments for $F28/F25$; follow a similar trend as Pu239 Jezebel. The lower GCFs are primarily an artificial effect due to the lack of experimental data for $F49/F25$ having for Pu239 Jezebel GCFs as large as 0.8, Table 14 below.

Table 8: Pu Flattop results

| $C/E \rightarrow$ Integral parameter \downarrow | Prior | | Posterior | |
|--|----------|-------|-----------|-------|
| | JEFF-3.3 | TENDL | JEFF-3.3 | TENDL |
| $F28/F25$ | 0.953 | 0.926 | 0.978 | 0.991 |
| $F37/F25$ | 0.991 | 0.987 | 1.014 | 1.026 |
| χ^2 | 9.4 | 23.2 | 2.5 | 2.1 |
| GCF | | | 0.45 | 0.48 |

| Integral parameter | Benchmark $E \pm \Delta E$ | | | Prior $C \pm \Delta C$ | | Posterior $C \pm \Delta C$ | |
|--------------------|-------------------------------|---------|------------|---------------------------|---------|-------------------------------|---------|
| | | | | JEFF-3.3 | TENDL | JEFF-3.3 | TENDL |
| $F28/F25$ | E | 0.17990 | C | 0.17142 | 0.16655 | 0.17595 | 0.17826 |
| | ΔE | 0.00200 | ΔC | 0.00530 | 0.00349 | 0.00250 | 0.00226 |
| $F37/F25$ | E | 0.85610 | C | 0.84871 | 0.84510 | 0.86845 | 0.87852 |
| | ΔE | 0.01200 | ΔC | 0.01934 | 0.01392 | 0.00798 | 0.00860 |

The results for ZPPR-9, the additional configuration for which spectral indices are assimilated, indicate, Table 9, that the GCF is smaller than for Godiva, compare with Table 3. This effect can primarily be ascribed to k_{eff} which is characterized by a GCF in the order of 0.2, Table 14 below. This low value largely originates from by far too weak reduction of the nuclear data uncertainty as a result of the adjustment, leading to disagreement between posterior ΔC and ΔE .

Table 9: ZPPR-9 results

| $C/E \rightarrow$ Integral parameter \downarrow | Prior | | Posterior | |
|--|----------|---------|-----------|---------|
| | JEFF-3.3 | TENDL | JEFF-3.3 | TENDL |
| $F28/F25$ | 0.954 | 0.909 | 0.999 | 1.000 |
| $F49/F25$ | 0.987 | 0.980 | 1.001 | 1.000 |
| $C28/F25$ | 0.967 | 0.997 | 1.000 | 1.000 |
| k_{eff} | 1.00793 | 1.00320 | 0.99853 | 0.99688 |
| χ^2 | 13.1 | 5.0 | 0.4 | 1.8 |
| GCF | | | 0.71 | 0.58 |

| Integral parameter | Benchmark $E \pm \Delta E$ | | | Prior $C \pm \Delta C$ | | Posterior $C \pm \Delta C$ | |
|--------------------|-------------------------------|---------|------------|---------------------------|---------|-------------------------------|---------|
| | | | | JEFF-3.3 | TENDL | JEFF-3.3 | TENDL |
| $F28/F25$ | E | 0.02070 | C | 0.01976 | 0.01882 | 0.02067 | 0.02070 |
| | ΔE | 0.00056 | ΔC | 0.00088 | 0.00033 | 0.00040 | 0.00030 |
| $F49/F25$ | E | 0.92250 | C | 0.91033 | 0.90437 | 0.92376 | 0.92257 |
| | ΔE | 0.01845 | ΔC | 0.03770 | 0.01630 | 0.01350 | 0.01132 |
| $C28/F25$ | E | 0.12960 | C | 0.12536 | 0.12927 | 0.12954 | 0.12965 |
| | ΔE | 0.00246 | ΔC | 0.00545 | 0.00125 | 0.00218 | 0.00109 |
| k_{eff} | E | 1.00106 | C | 1.00900 | 1.00427 | 0.99959 | 0.99794 |
| | ΔE | 0.00117 | ΔC | 0.01117 | 0.01061 | 0.00994 | 0.00953 |

The results for ZPR-6/7, another compound system with sodium, Table 10, do not reproduce in this case the trend of adjustment efficiency so far observed for $F28/F25$. The improved χ^2 as a result of the adjustment is rather attributable to k_{eff} , Table 2. The lower GCF as compared to ZPPR-9 reproduces though the similar trend of a larger JEFF-3.3 value.

Table 10: ZPR-6/7 results

| $C/E \rightarrow$ Integral parameter \downarrow | Prior | | Posterior | |
|--|----------|---------|-----------|---------|
| | JEFF-3.3 | TENDL | JEFF-3.3 | TENDL |
| $F28/F25$ | 1.015 | 0.962 | 1.060 | 1.058 |
| $F49/F25$ | 0.967 | 0.960 | 0.980 | 0.980 |
| $C28/F25$ | 0.975 | 1.005 | 1.008 | 1.007 |
| k_{eff} | 1.00862 | 1.00777 | 0.99839 | 0.99834 |
| χ^2 | 4.5 | 4.2 | 1.4 | 1.3 |
| GCF | | | 0.48 | 0.40 |

| Integral parameter | Benchmark $E \pm \Delta E$ | | | Prior $C \pm \Delta C$ | | Posterior $C \pm \Delta C$ | |
|--------------------|-------------------------------|---------|------------|---------------------------|---------|-------------------------------|---------|
| | | | | JEFF-3.3 | TENDL | JEFF-3.3 | TENDL |
| $F28/F25$ | E | 0.02230 | C | 0.02263 | 0.02146 | 0.02364 | 0.02359 |
| | ΔE | 0.00067 | ΔC | 0.00097 | 0.00037 | 0.00043 | 0.00034 |
| $F49/F25$ | E | 0.94350 | C | 0.91197 | 0.90564 | 0.92501 | 0.92469 |
| | ΔE | 0.01981 | ΔC | 0.03702 | 0.01620 | 0.01320 | 0.01122 |
| $C28/F25$ | E | 0.13230 | C | 0.12899 | 0.13296 | 0.13332 | 0.13320 |
| | ΔE | 0.00318 | ΔC | 0.00549 | 0.00128 | 0.00218 | 0.00112 |
| k_{eff} | E | 1.00051 | C | 1.00914 | 1.00828 | 0.99890 | 0.99885 |
| | ΔE | 0.00230 | ΔC | 0.01088 | 0.01074 | 0.00985 | 0.00976 |

The JOYO MK-I 64 F/A results, Table 11, indicate a particularly large GCF obtained using TENDL data due to agreement reached between posterior k_{eff} and experiment.

Table 11: JOYO MK-I 64 F/A results

| $C/E \rightarrow$ Integral parameter \downarrow | Prior | | Posterior | |
|--|----------|---------|-----------|---------|
| | JEFF-3.3 | TENDL | JEFF-3.3 | TENDL |
| k_{eff} | 1.00804 | 1.02025 | 0.99369 | 0.99856 |
| χ^2 | 1.3 | 8.2 | 0.8 | 0.0 |
| GCF | | | 0.67 | 0.90 |

| Integral parameter | Benchmark $E \pm \Delta E$ | | | Prior $C \pm \Delta C$ | | Posterior $C \pm \Delta C$ | |
|--------------------|-------------------------------|---------|------------|---------------------------|---------|-------------------------------|---------|
| | | | | JEFF-3.3 | TENDL | JEFF-3.3 | TENDL |
| k_{eff} | E | 0.99210 | C | 1.00008 | 1.01219 | 0.98584 | 0.99067 |
| | ΔE | 0.00700 | ΔC | 0.01556 | 0.00704 | 0.01104 | 0.00809 |

The results for SNEAK 7A, a compound system without sodium, show, Table 12, that the adjustment appears efficient particularly for $F28/F25$ and k_{eff} . However, there is disagreement between posterior ΔC s and ΔE s leading to a GCF smaller than 0.5 despite posterior χ^2 s approaching 1. The observed uncertainty reduction appears on the one hand too pronounced for the spectral indices; on the other hand it results too mild for k_{eff} .

Table 12: SNEAK 7A results

| $C/E \rightarrow$ Integral parameter \downarrow | Prior | | Posterior | |
|--|----------|---------|-----------|---------|
| | JEFF-3.3 | TENDL | JEFF-3.3 | TENDL |
| $F28/F25$ | 0.921 | 0.886 | 0.957 | 0.959 |
| $F49/F25$ | 0.959 | 0.959 | 0.975 | 0.977 |
| $C28/F25$ | 0.934 | 0.961 | 0.966 | 0.965 |
| k_{eff} | 1.00740 | 1.00865 | 0.99800 | 0.99773 |
| χ^2 | 3.8 | 4.9 | 0.9 | 0.9 |
| GCF | | | 0.48 | 0.42 |

| Integral parameter | Benchmark $E \pm \Delta E$ | | | Prior $C \pm \Delta C$ | | Posterior $C \pm \Delta C$ | |
|--------------------|-------------------------------|---------|------------|---------------------------|---------|-------------------------------|---------|
| | | | | JEFF-3.3 | TENDL | JEFF-3.3 | TENDL |
| $F28/F25$ | E | 0.04490 | C | 0.04135 | 0.03976 | 0.04297 | 0.04306 |
| | ΔE | 0.00153 | ΔC | 0.00180 | 0.00066 | 0.00077 | 0.00056 |
| $F49/F25$ | E | 1.02300 | C | 0.98078 | 0.98110 | 0.99709 | 0.99903 |
| | ΔE | 0.03069 | ΔC | 0.03980 | 0.01701 | 0.01437 | 0.01112 |
| $C28/F25$ | E | 0.13800 | C | 0.12895 | 0.13260 | 0.13330 | 0.13321 |
| | ΔE | 0.00428 | ΔC | 0.00552 | 0.00142 | 0.00228 | 0.00119 |
| k_{eff} | E | 1.00380 | C | 1.01123 | 1.01248 | 1.00179 | 1.00152 |
| | ΔE | 0.00400 | ΔC | 0.01016 | 0.00958 | 0.00899 | 0.00832 |

Finally, the SNEAK 7B results are provided in Table 13 showing efficient adjustments qualitatively similar to SNEAK 7A. The larger GCF obtained using JEFF-3.3 data can mostly be attributed to less pronounced spectral index discrepancies between posterior ΔC s and ΔE s.

Table 13: SNEAK 7B results

| $C/E \rightarrow$ Integral parameter \downarrow | Prior | | Posterior | |
|--|----------|---------|-----------|---------|
| | JEFF-3.3 | TENDL | JEFF-3.3 | TENDL |
| $F28/F25$ | 0.955 | 0.905 | 1.005 | 0.986 |
| $F49/F25$ | 0.989 | 0.980 | 1.014 | 0.998 |
| $C28/F25$ | 0.960 | 0.996 | 0.997 | 0.997 |
| k_{eff} | 1.00832 | 1.00246 | 1.00013 | 0.99764 |
| χ^2 | 2.1 | 4.3 | 0.1 | 0.2 |
| GCF | | | 0.74 | 0.64 |

| Integral parameter | Benchmark $E \pm \Delta E$ | | | Prior $C \pm \Delta C$ | | Posterior $C \pm \Delta C$ | |
|--------------------|-------------------------------|---------|------------|---------------------------|---------|-------------------------------|---------|
| | | | | JEFF-3.3 | TENDL | JEFF-3.3 | TENDL |
| $F28/F25$ | E | 0.03280 | C | 0.03133 | 0.02967 | 0.03296 | 0.03235 |
| | ΔE | 0.00079 | ΔC | 0.00151 | 0.00052 | 0.00074 | 0.00045 |
| $F49/F25$ | E | 1.01400 | C | 1.00274 | 0.99404 | 1.02784 | 1.01188 |
| | ΔE | 0.02028 | ΔC | 0.04519 | 0.01915 | 0.01610 | 0.01298 |
| $C28/F25$ | E | 0.13200 | C | 0.12667 | 0.13146 | 0.13162 | 0.13159 |
| | ΔE | 0.00475 | ΔC | 0.00615 | 0.00151 | 0.00253 | 0.00131 |
| k_{eff} | E | 1.00280 | C | 1.01114 | 1.00527 | 1.00293 | 1.00043 |
| | ΔE | 0.00450 | ΔC | 0.01080 | 0.00965 | 0.00915 | 0.00819 |

By looking at the entirety of data, Tables 3-13, in a more global manner, it is observed that uncertainties of the computed parameters resulting from nuclear data uncertainties are indeed reduced through the adjustment according to the general experience; however, the strength of this reduction may vary from case to case.

Table 14 summarizes the GCFs for the target parameters in order to provide a clearer overview.

Table 14: Summary of the GCFs with arithmetic means

| Configuration | Integral parameter | GCF | |
|----------------------------|--------------------|----------|-------|
| | | JEFF-3.3 | TENDL |
| Godiva | <i>F28/F25</i> | 0.98 | 0.95 |
| | <i>F49/F25</i> | 0.88 | 0.91 |
| | <i>F37/F25</i> | 0.87 | 0.74 |
| | Mean | 0.91 | 0.87 |
| U235 Flattop | <i>F28/F25</i> | 0.95 | 0.73 |
| | <i>F49/F25</i> | 0.72 | 0.92 |
| | <i>F37/F25</i> | 0.65 | 0.67 |
| | Mean | 0.77 | 0.77 |
| Big Ten | <i>F28/F25</i> | 0.41 | 0.22 |
| | <i>F49/F25</i> | 0.32 | 0.44 |
| | <i>F37/F25</i> | 0.34 | 0.91 |
| | <i>C28/F25</i> | 0.45 | 0.30 |
| | Mean | 0.38 | 0.47 |
| Pu239 Jezebel | <i>F28/F25</i> | 0.37 | 0.86 |
| | <i>F49/F25</i> | 0.78 | 0.67 |
| | <i>F37/F25</i> | 0.72 | 0.26 |
| | Mean | 0.62 | 0.60 |
| Pu240 Jezebel | <i>F28/F25</i> | 0.29 | 0.75 |
| | <i>F37/F25</i> | 0.18 | 0.02 |
| | Mean | 0.23 | 0.38 |
| Pu Flattop | <i>F28/F25</i> | 0.37 | 0.70 |
| | <i>F37/F25</i> | 0.52 | 0.27 |
| | Mean | 0.45 | 0.48 |
| ZPPR-9 | <i>F28/F25</i> | 0.84 | 0.71 |
| | <i>F49/F25</i> | 0.85 | 0.77 |
| | <i>C28/F25</i> | 0.94 | 0.73 |
| | k_{eff} | 0.23 | 0.23 |
| | Mean | 0.71 | 0.58 |
| ZPR-6/7 | <i>F28/F25</i> | 0.22 | 0.19 |
| | <i>F49/F25</i> | 0.55 | 0.50 |
| | <i>C28/F25</i> | 0.78 | 0.52 |
| | k_{eff} | 0.39 | 0.40 |
| | Mean | 0.48 | 0.40 |
| JOYO MK-I 64 F/A | k_{eff} | 0.67 | 0.90 |
| SNEAK 7A | <i>F28/F25</i> | 0.37 | 0.32 |
| | <i>F49/F25</i> | 0.49 | 0.43 |
| | <i>C28/F25</i> | 0.44 | 0.30 |
| | k_{eff} | 0.62 | 0.64 |
| | Mean | 0.48 | 0.42 |
| SNEAK 7B | <i>F28/F25</i> | 0.91 | 0.64 |
| | <i>F49/F25</i> | 0.69 | 0.78 |
| | <i>C28/F25</i> | 0.70 | 0.45 |
| | k_{eff} | 0.67 | 0.69 |
| | Mean | 0.74 | 0.64 |
| Mean of target experiments | | 0.56 | 0.57 |

A first observation is that the overall mean values, last row of the table, are almost equal, similarly to the χ^2 s provided in Table 2, supporting that the overall adjustment efficiency, of course in the specific case of the APIA

methodology used in conjunction with the current limited database for assimilations, is comparable between JEFF-3.3 and TENDL data for the selected target experiments.

However, there are compensation effects for the individual parameters especially as regards the Pu metal systems and Big Ten. For example the Pu239 Jezebel coverage factor of $F28/F25$ is respectively 0.37 and 0.86 in the case of JEFF-3.3 and TENDL data; whereas, on the contrary, the GCFs are respectively 0.72 and 0.26 for $F37/F25$, causing, for this configuration, compensations corresponding to the χ^2 s. Also consistently with the χ^2 s, Pu240 Jezebel and Big Ten are seen deviating more significantly from the overall means as compared to the other configurations, giving lower coverage factors.

Of particular interest is $C28/F25$ for Big Ten having the same posterior χ^2 of 2.0, Table 2, along with a much larger coverage factor in the case of JEFF-3.3 data (0.45 versus 0.30) confirming that different trends are possible between GCFs and χ^2 s. That e.g. the GCF obtained for $F28/F25$ on the basis of JEFF-3.3 data is larger can be deduced from Fig. 7: in fact it is seen that the JEFF-3.3 coverage factor resulting from the superposition of green and violet includes almost completely the TENDL coverage factor given by the superposition of yellow and violet. The efficiency of the adjustment is also deducible from the indicated prior values and the means of the posterior PDFs.

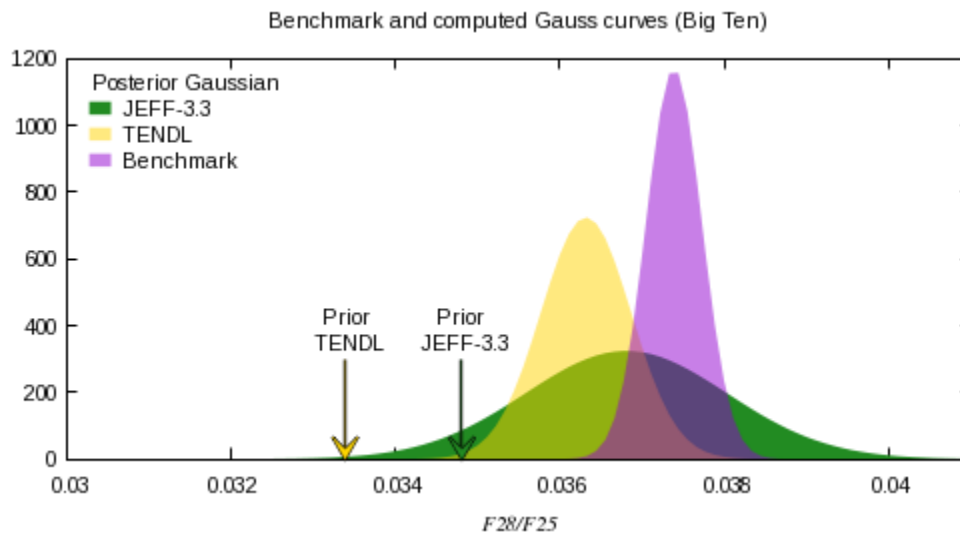


Fig. 7: Illustrative data for (posterior) GCFs

As previously highlighted for the fission cross-section of U235, GCFs of individual cross-sections may be viewed as “distances” of these cross-sections. In this way, “distances” between prior data stemming from different data sources, can be compared with corresponding “distances” between posterior data on the one-to-one basis. The larger is the GCF the lower is the “distance”. In the limiting cases, if the GCF is one, the “distance” would be zero indicating full data agreement. On the other hand, if the coverage factor is zero, the “distance” may be assumed infinite. Correspondingly, data is provided in Table 15.

Table 15: GCFs of JEFF-3.3 and TENDL data along with arithmetic means

| Nuclide → | O16 | Na23 | Cr52 | Fe56 | Ni58 | U235 | U238 | Pu239 | Pu240 | Pu241 |
|--|------|------|------|------|------|------|------|-------|--------------|-------|
| Cross-section or fission neutron yield ↓ | | | | | | | | | | |
| Prior GCF, mean of group-wise data | | | | | | | | | | |
| Elastic scattering | 0.55 | 0.32 | 0.12 | 0.48 | 0.35 | 0.49 | 0.44 | 0.35 | 0.50 | 0.32 |
| Inelastic scattering | 0.53 | 0.34 | 0.25 | 0.52 | 0.26 | 0.33 | 0.37 | 0.43 | 0.56 | 0.22 |
| Capture | 0.12 | 0.42 | 0.39 | 0.62 | 0.50 | 0.18 | 0.50 | 0.27 | 0.34 | 0.25 |
| (n, xn) | 0.58 | 0.44 | 0.0 | 0.0 | 0.23 | 0.22 | 0.25 | 0.16 | 0.65 | 0.36 |
| Fission | - | - | - | - | - | 0.36 | 0.42 | 0.44 | 0.21 | 0.37 |
| $\bar{\nu}$ | - | - | - | - | - | 0.28 | 0.14 | 0.29 | ^a | 0.50 |
| Mean | 0.44 | 0.38 | 0.19 | 0.40 | 0.33 | 0.31 | 0.35 | 0.32 | 0.45 | 0.34 |
| Mean of nuclides | 0.35 | | | | | | | | | |
| Posterior GCF, mean of group-wise data | | | | | | | | | | |
| Elastic scattering | 0.40 | 0.38 | 0.14 | 0.61 | 0.30 | 0.48 | 0.41 | 0.35 | 0.50 | 0.33 |
| Inelastic scattering | 0.53 | 0.39 | 0.26 | 0.54 | 0.29 | 0.20 | 0.35 | 0.34 | 0.57 | 0.23 |
| Capture | 0.13 | 0.42 | 0.42 | 0.62 | 0.50 | 0.16 | 0.44 | 0.28 | 0.26 | 0.27 |
| (n, xn) | 0.55 | 0.34 | 0.0 | 0.0 | 0.24 | 0.22 | 0.24 | 0.15 | 0.64 | 0.32 |
| Fission | - | - | - | - | - | 0.29 | 0.39 | 0.38 | 0.27 | 0.37 |
| $\bar{\nu}$ | - | - | - | - | - | 0.28 | 0.14 | 0.31 | ^a | 0.51 |
| Mean | 0.40 | 0.33 | 0.20 | 0.44 | 0.33 | 0.27 | 0.33 | 0.30 | 0.45 | 0.34 |
| Mean of nuclides | 0.34 | | | | | | | | | |

^a JEFF-3.3 covariance data is not available in this case.

It is observed that prior and posterior means of GCFs are similar for the nuclides taking part in the adjustment. Therefore the “distance” between JEFF-3.3 and TENDL data is globally not changing as a consequence of the assimilation. However, keeping in mind that variances are reduced by the adjustment, posterior cross-sections along with fission neutron yields, in a global sense, must get closer to each other as compared to the prior situation, which is a promising result: the adjusted cross-sections indicate the tendency of converging to similar values (with the usual meaning) for JEFF-3.3 and TENDL data. The simple geometric explanation is that since normal probability density functions having lower variances are narrower, the means of the posterior PDFs must approach relatively to the prior PDFs in order to preserve the coverage factor. However, the current, limited assimilation database does not succeed in reproducing a similar trend for the variances since the coverage factor is not increased by the adjustment.

In addition, Fig. 8 shows energy dependent GCFs in the specific case of the fission cross-section of U235 for which the prior and posterior means of the 33 group coverage factors are respectively 0.36 and 0.29, Table 15 above. That the prior mean should be higher, in this case, is supported by the figure; it is also seen in spite of much larger differences for individual groups between posterior and prior GCFs, that there are largely compensation effects which prevents identifying meaningful trends between prior and posterior situations.

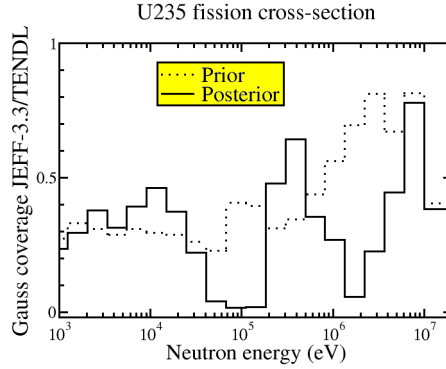


Fig. 8: Illustrative energy dependent GCFs

4. Conclusions and recommendations

This study has dealt with adjustments obtained by means of the Asymptotic Progressing Incremental nuclear data Aadjustment (APIA) methodology (Pelloni and Rochman, 2018). When using this method the adjustment is made progressively in subsequent steps, by considering at a time small groups of well documented experiments possibly with low experimental uncertainties, which have been performed in the same configuration. More specifically, six integral parameters which are the Godiva and ZPPR-9 central spectral indices were considered in the current data assimilation obtained with consistent JEFF-3.3 and TENDL based data. The word consistent is used here to indicate that data along with their covariances are all stemming from the same source and were also processed in a consistent manner. Only under this circumstance along with the absence of multiplication factors in the assimilation database, APIA simulations are supposed leading to credible adjustments (Pelloni and Rochman, 2018). Consistently with these requirements, target experiments including multiplication factors were chosen primarily based upon the availability in the ICSBEP and IRPhEP databases (Briggs, 2004), (Nuclear Energy Agency (NEA), 2017) of configurations in which spectral indices were measured; largely including the integral parameters analyzed in the framework of the International “Subgroup 39” on “Methods and approaches to provide feedback from nuclear and covariance data adjustment for improvement of nuclear data files” of the Working Party on Evaluation Cooperation (WPEC) of the OECD Nuclear Energy Agency Nuclear Science Committee (NSC) (Salvatores et al., 2014).

The selection led to 34 target experiments including the six mentioned integral parameters which were part of the assimilation. 11 different experimental configurations are involved, Table 1, including fast-spectrum metal systems using U and Pu fuel, Los Alamos critical spheres one of which is Godiva, as well as more complex fast-spectrum compound systems with sodium, such as ZPPR-9 simulating liquid metal fast reactors, and also without sodium i.e. the SNEAK facility. The target experiments were investigated on the basis of the resulting posterior data, more precisely adjusted data along with their covariances, in addition to prior unadjusted data.

It has been shown that despite the limited assimilation database, just 6 well documented experiments with uncertainties of the order of 1-2%, the adjustment is efficient: the mean χ^2 of the 34 experiments computed with adjusted instead of unadjusted JEFF-3.3 and TENDL data was subject to strong reductions resulting in values smaller than 2, Table 2, compared to prior values of respectively 4.1 and 14.7. This promising outcome could be obtained by tightening the convergence criterion in the APIA simulations by requiring that the relative cross-section difference between two successive within step iterations does not exceed let say 0.01% , previously 1% (Pelloni and Rochman, 2018); the ratios C/E s of the computed (C) to experimental (E) values were thus forced to approach more closely unity for the assimilated integral parameters. Correspondingly, the posterior covariance data was reassessed in order to avoid multiple considerations of the experimental information in the data assimilation, by using the prior instead of posterior covariance matrix in one of the proposed Generalized Linear Least-Squares (GLLS) equations, as in Eq. (1) above.

The adjustment performance has been additionally assessed on the basis of more general principles by assuming that nuclear data along with their covariances are an inseparable, unique entity, which is viewed as a general, indispensable constraint for future work in general; agreement in the posterior situation between C s and E s has been investigated by accounting for the resulting associated uncertainties, ΔC , due to nuclear data uncertainties, in a statistical way. This approach also allowed comparing data from different sources, currently JEFF-3.3 and TENDL, on the one-to-one basis also providing a link between prior and posterior situations.

It has been proposed that the posterior C s viewed as adjusted expectation or mean values, along with their (adjusted) uncertainties due to nuclear data uncertainties, ΔC s, in fact standard deviations or square roots of variances, are systematically compared with the corresponding benchmark means, E s, along with variances corresponding to their uncertainties, ΔE s. In the specific case of this study using the GLLS approximation, the comparison occurred in terms of Gaussian Coverage Factors, GCFs, on the basis of the normal Probability Density Functions, PDFs, having these means and variances. In general situations, it was felt that the assumption of normal PDFs depends on the specific assimilation methodology, e.g. deterministic or stochastic (Rochman et al., 2018), and is not necessarily suited.

More precisely, the GCF of two data sets consisting each of one mean along with its variance, a number between 0 and 1, is given by the common surface spanned below the normal PDFs associated with each set having these means and variances, Fig. 1. For simplicity, the GCF was referred to as coverage factor of the means.

Larger posterior GCFs of C s and E s are targeted; the GCF thus provides a degree of suitability of the prior covariance data in generating posterior data through the data assimilation process. The larger is the posterior GCF obtained, the more reliable seems the prior covariance data in obtaining posterior data.

Correspondingly, since the mean posterior GCFs of the 34 target experiments are almost identical, Table 14, similarly to the χ^2 s, Table 2, important conclusions of this study are that

- (1) the efficiency and performance of the adjustment is comparable between JEFF-3.3 and TENDL data for the 34 experiments analyzed, and

underlining a previous statement,

- (2) improved performance as compared to the prior situation can be achieved by just assimilating data of a few well documented experiments with low uncertainties.

The statistical approach has though indicated compensation effects for the individual parameters especially as regards the Pu metal systems and Big Ten. For example, Table 14, the Pu239 Jezebel coverage factor of $F28/F25$ is respectively 0.37 and 0.86 in the case of JEFF-3.3 and TENDL data; whereas, on the contrary, the GCFs are respectively 0.72 and 0.26 for $F37/F25$, causing, for this configuration, compensations corresponding to the χ^2 s, Table 2. Also consistently with the χ^2 s, Pu240 Jezebel and Big Ten were seen deviating more significantly from the overall means as compared to the other configurations, giving lower coverage factors. Of particular interest is $C28/F25$ for Big Ten having the same posterior χ^2 of 2.0, Table 2, along with a much larger coverage factor in the case of JEFF-3.3 data (0.45 versus 0.30) showing that different trends are in principle possible between GCFs and χ^2 s.

It has been recognized that GCFs of individual cross-sections may additionally be used to characterize “distances” between prior data stemming from different sources (Varet et al., 2015.), allowing then comparing these “distances” with corresponding “distances” obtained in the posterior situation on the one-to-one basis. The larger is the GCF the lower is this “distance”.

It has been found, last part of Section 3 that the “distance” of JEFF-3.3 and TENDL data which is associated with the mean coverage factor, Table 15, is not changing as a consequence of the assimilation. However, since the variances are reduced by the adjustment, another important conclusion could be reached, namely that

(3) adjusted cross-sections tend to converge to similar values by comparing JEFF-3.3 and TENDL data.

The simple geometric explanation of this finding is that since normal probability density functions having lower variances are narrower, the means of the posterior PDFs must approach relatively to the prior PDFs in order to preserve the coverage factor. However, the current, limited assimilation database was not able reproducing a similar trend for the variances, since the coverage factor is not increased by the adjustment.

It is recommended that the nuclear data cross-correlations should be studied and involved more closely in these kinds of comparisons. However, a suited methodology needs to be developed. It is felt that even more important is to study the effect of enlarged databases on all these results, to include additional data sources e.g. ENDF/B-VIII, and last but not least to investigate whether the adjustment trends of the C/E s currently assessed based upon APIA simulations carried out with ERANOS are reproducible with a stochastic code.

5. Acknowledgments

The authors wish herewith to acknowledge the individual members of “Subgroup 39” on “Methods and approaches to provide feedback from nuclear and covariance data adjustment for improvement of nuclear data files” of the Working Party on Evaluation Cooperation (WPEC) of the OECD Nuclear Energy Agency Nuclear Science Committee (Subgroup webpage) for their fruitful discussions during the various meetings, especially the coordinators, Massimo Salvatores and Giuseppe Palmiotti. The authors are particularly indebted to Oscar Cabellos for having generated the JEFF-3.3 based covariance data which has been repeatedly used in this study. Stimulating discussions at PSI with Konstantin Mikityuk in the framework of the FAST and ESFR-SMART projects, and also with Andreas Pautz, were also appreciated.

References

- Briggs, J. B., Editor, 2014: International Handbook of evaluated Criticality Safety Benchmark Experiments, Organization for Economic Co-operation and Development, Nuclear Energy Agency, NEA/NSC/DOC(95)03/I.
- Cacuci, G., Editor, 2010: Handbook of Nuclear Engineering, Volume 3, Chapter 17, Springer Science+Business Media LLC 2010, ISBN: 978-0-387-98130-7.
- Koning, A. and Rochman, D., 2008: Towards sustainable nuclear energy: Putting nuclear physics to work, Annals of Nuclear Energy, 35, 2024.
- Koning, A. and Rochman, D., 2012: Modern nuclear data evaluation with the TALYS code system, Nuclear Data Sheets, 113, 2841.
- MacFarlane, R. E., et al., 2012: The NJOY Nuclear Data Processing System, Version 2012, LA-UR-12-27079 Rev, edited by Kahler, A. C., Los Alamos National Laboratory, URL <http://t2.lanl.gov/nis/codes/NJOY12/NJOY2012.82.pdf>
- Nuclear Energy Agency (NEA), 2017: International Handbook of Evaluated Physics Benchmark Experiments, Organization for Economic Co-operation and Development, Nuclear Energy Agency, NEA/NSC/DOC(2006)1.
- Nuclear Energy Agency (NEA), 2018, URL <http://www.oecd-nea.org/dbdata/jeff/jeff33>
- Pelloni, S., 2014: Application of an iterative methodology for cross-section and variance/covariance data adjustment to the analysis of fast spectrum systems, Annals of Nuclear Energy, 72, 373.
- Pelloni, S., 2017: Comparison of progressive incremental adjustment sequences for cross-section and variance/covariance data adjustment by analyzing fast-spectrum systems, Annals of Nuclear Energy, 106, 33.
- Pelloni, S. and Rochman, D., 2018: Cross-section adjustment in the fast energy range on the basis of an Asymptotic Progressing nuclear data Incremental Adjustment (APIA) methodology, Annals of Nuclear Energy, 115, 323.
- Rimpault, G. et al., 2002: The ERANOS data and code system for fast reactor neutronic analyses. In: Proceedings of the International Conference on the New Frontier of Nuclear Technology: Reactor Physics, Safety and High-Performance Computing (PHYSOR 2002), Seoul, Korea.
- Rochman, D. et al., 2016: Nuclear data uncertainty for criticality safety: Monte Carlo vs. linear perturbation, Annals of Nuclear Energy 92, 150.
- Rochman, D. et al., 2018: How inelastic scattering stimulates nonlinear reactor core parameter behavior, Annals of Nuclear Energy 112, 236.
- Salvatores, M. et al., 2014: Methods and Issues for the Combined Use of Integral Experiments and Covariance Data: Results of a NEA International Collaborative Study, Nuclear Data Sheets, 118, 38.
- Varet S. et al., 2015: Quality quantification of evaluated cross section covariances, Nuclear Data Sheets 123, 191.